NEW SIGMOID CURVES: BEYOND THE TRADITIONAL LOGISTIC MODELS

NUEVAS CURVAS SIGMOIDALES: MÁS ALLÁ DE LOS MODELOS LOGÍSTICOS TRADICIONALES

M. T. Pérez-Maldonado[a†], J. Bravo-Castillero[b], R. Mansilla[c], R. O. Caballero-Pérez[d]

a) Department of Theoretical Physics. Physics Faculty, University of Havana, mtperez@fisica.uh.cu†
b) UA-IIMAS-EY, Universidad Nacional Autónoma de México
c) CEPHCIS-CEIICH, Universidad Nacional Autónoma de México
d) Independent researcher
† corresponding author

Recibido 4/3/2025; Aceptado 15/6/2025

S-shaped or sigmoid curves can be defined as the solutions of autonomous first-order differential equations that satisfy four conditions. Without solving the equations, we demonstrate that the solutions of the logistic family and the Smith-Birch model satisfy these conditions. We introduce two generalizations of the Smith-Birch, whose solutions are identified as S-shaped for some range of variation of the parameters. The new models introduced here predict the spread of the disease better than traditional logistic family models for time series of the cumulative number of cases for the first 61 days of the COVID-19 pandemic in some countries.

Las curvas en forma de S o curvas sigmoidales pueden definirse como soluciones de ecuaciones diferenciales autónomas de primer orden que cumplen con cuatro condiciones, a través de las cuales se demuestra sin necesidad de resolverlos que los modelos de la familia logística generalizada y el de Smith-Birch tienen soluciones sigmoidales. Se introducen dos generalizaciones del modelo de Smith-Birch, cuyas soluciones son curvas sigmoidales para cierto rango de variación de los parámetros. Se encontraron series temporales del número cumulativo de casos para los 61 primeros días de la pandemia de COVID-19 en algunos países donde los nuevos modelos aquí introducidos predicen mejor la propagación de la enfermedad que los modelos tradicionales de la familia logística.

Keywords: Complex systems modelling (Modelado de sistemas complejos); Sigmoid curves (Curvas sigmoideas); Growth models (Modelos de crecimiento); Data fitting (Ajuste de datos); Forecast (Pronóstico).

I. INTRODUCTION

S-shaped, or sigmoid curves (SC) can be found frequently in sciences, including physics and complex systems. Their ubiquity arises from their ability to approximate step-like behaviors in a continuous and differentiable manner. The S-shape is a consequence of competition between positive feedback, which tends to produce exponential growth, and negative feedback, which produces saturation or stabilization due to limiting factors. Some paradigmatic examples of SC are the Fermi-Dirac distribution function and the magnetization in a system of two-state (spin 1/2) particles.

SC are observed in a wide variety of phenomena and have a large number of applications. For example, in computational sciences [1], neuro and behavioral sciences [2–6], molecular biology [7], chemistry [8, 9], agricultural, livestock and veterinary sciences [10–14], pedology [15], ecology [16–18], economics and marketing [19, 20], electronics [21], materials engineering [22–24], spectroscopy [25] and autonomous driving [26]. An exhaustive review of more applications can be found in [27].

Applications of SC in epidemiology deserve a special mention. The cumulative number of cases in the early stages of epidemics frequently exhibits a sigmoid growth behavior. See, for example [28–44]. Sigmoid curves can be described as solutions of first-order differential equations of the form:

$$\frac{dN}{dt} = g_{\mathbf{\Pi}}(N) \tag{1}$$

where the function $g_{\mathbf{\Pi}}(N)$ with parameter vector $\mathbf{\Pi} = \{\Pi_1, \Pi_2, \cdots \Pi_k\}$ must satisfy the conditions [45]:

I. $g_{\mathbf{\Pi}}(N)$ is C^1 over the interval $[f, c]$, with $0 \leq f < c$.

II. $g_{\mathbf{\Pi}}(f) = g_{\mathbf{\Pi}}(c) = 0$.

III. $g_{\mathbf{\Pi}}(N) > 0$ if $N \in (f, c)$.

IV. $\operatorname{sgn}(g'_{\mathbf{\Pi}}(N)) = \begin{cases} 1 & \text{if} \quad N \in [f, N^*) \\ -1 & \text{if} \quad N \in (N^*, c] \end{cases}$
where $N^* \in (f, c)$.

Condition I guarantees that for each point $\Pi^* \in \mathbb{R}^k$, there exists a unique integral curve $N = N(t, \Pi^*)$ (i.e., the graph of a non-prolongable solution) of equation (1) passing through each point (t_0, N_0) of an open set contained in the strip $\mathbb{R}\times(f, c)$ (Section 4.4, Chapter 4, [46]). Property III ensures that the solution $N = N(t, \Pi^*)$ is an increasing function, while property IV implies the existence of a unique inflection point (t^*, N^*) of the solution curve that marks accelerated growth between f and N^*, and decelerated or retarded growth between N^* and c. Condition II ensures that the stationary solutions defined by the equilibrium positions f and c determine the lower and

upper limits, respectively, of the dynamics of interest. In this way, conditions (I-IV) guarantee the existence of S-shaped solutions. Furthermore, under conditions (I-IV), equation (1) only has equilibrium positions at the endpoints of the interval, and these points cannot collapse, which means that the parameters with the positiveness conditions considered in III and IV do not bifurcate.

Equation (1) is separable, so it is solvable at least for t as a function of N:

$$t - t_0 = \int_{N_0}^{N} \frac{dN}{g\Pi(N)} \tag{2}$$

where $N(t_0) = N_0$ is the initial condition. In some particular cases it is possible to obtain N as an explicit function of t.

Different analytic and numerical methods have been used to study SC [47–51].

II. THE LOGISTIC FAMILY

The simplest sigmoid growth model is the logistic model, also known as the Verhulst model [52], a two-parameter, second-order approximation of (1)

$$\frac{dN}{dt} = rN\left(1 - \frac{N}{K}\right) \tag{3}$$

Logistic model satisfies SC conditions (I-IV) for $f = 0$ and $c = K$. It exhibits an initial exponential growth with relative growth rate r and a saturation value or carrying capacity (horizontal asymptote) at $N = K$. The inflection point is $N^* = \frac{K}{2}$, which is fixed for a given value of K only. This is the main limitation of this model: more flexibility is needed for the inflection point in order to fit different datasets. In order to do that, several generalizations have been proposed as well as for flexibilizing other features of the SC [13, 53–56]. This generalization is achieved by including more parameters. In [53] a generalized five-parameter logistic model is proposed:

$$\frac{dN}{dt} = rN^{\alpha}\left(1 - \left(\frac{N}{K}\right)^{\beta}\right)^{\gamma} \tag{4}$$

where α, β and γ are positive real numbers. In what follows we shall call model (4) the Tsoularis generalized logistic model. Conditions (I-IV) are satisfied for these parameter values with $f = 0$, $c = K$ and $N^* = K(\gamma/(\gamma + \alpha\beta))^{1/\alpha}$, so the model has SC solutions. Parameter α allows non exponential initial growth, while β and γ, along with α, change the position of the inflection point. In general, α, β and γ are intended to smooth the equation (4) vector field.

Some well-known, particular cases of (4) are shown in the next table.

Model	α	β	γ
Logistic	1	1	1
Generalized Logistic	α	1	1
Richards	1	β	1
Generalized Richards	α	β	1
Gompertz	1	$\to 0$	1
Generalized Gompertz	α	$\to 0$	1

III. THE SMITH-BIRCH MODEL

A different, lesser-known kind of generalization for the logistic model was introduced by Smith [57] in order to correct problems associated with time lags in a food-limited population. Birch [58] arrived to the same result by introducing an alternative modification in the logistic model, trying to overcome some numerical unstabilities appearing in the Richards model when fitting experimental data:

$$\frac{dN}{dt} = \frac{rN(K - N)}{AN + K} \tag{5}$$

This three-parameter model reduces to the logistic model when $A = 0$ (furthermore, the case $A = -1$ corresponds to the exponential growth). When $A > 0$ Smith-Birch model satisfies conditions (I-IV) with $f = 0$, $c = K$ and $N^* = K(\sqrt{A+1} - 1)/A$, so it produces SC. In this way, A changes the position of the inflection point. In Figure 1 some solutions for this model are shown.

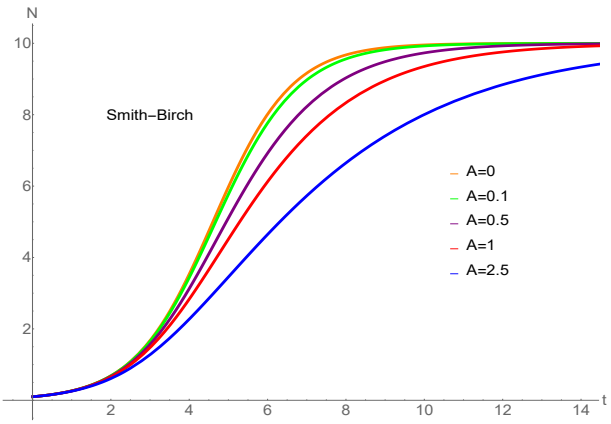

Figure 1. Smith-Birch model curves with $K = 10$, $N(0.01) = 0.1$ and $A = 0$ (orange), $A = 0.1$ (green), $A = 0.5$ (purple), $A = 1$ (red), $A = 2.5$ (blue). Inflection points correspond to $N^* = 5, 4.88, 4.49, 4.14, 3.48$, respectively.

IV. NEW SIGMOIDAL CURVES

In a previous work, partially published in [44], we applied several models of the logistic family to the time series for the cumulative number of cases during the first 61 days of the COVID 19 pandemic for 131 countries. We have found that some countries' data were not properly fitted with none of the models considered, so it is interesting to study some new, four-parameter generalizations of the Smith-Birch model:

$$\frac{dN}{dt} = \frac{rN(K-N)}{AN^p + K} \tag{6}$$

$$\frac{dN}{dt} = \frac{rN^p(K-N)}{AN + K} \tag{7}$$

which we will call Smith-Birch A and Smith-Birch B models, respectively. Both of these new models reduce to Smith-Birch when $p = 1$.

They satisfy conditions (I-III) for $A > 0$ with $f = 0$ and $c = K$. Condition IV requires a numerical analysis. Furthermore, it does not seem possible to find analytic expressions for the inflection point N^*. Hopefully, all these models, including (4), are analytically solvable for t as a function of N, using hypergeometric functions. See Appendix I for details. In Figures 2 and 3 some solutions for Smith-Birch A and Smith-Birch B models are shown.

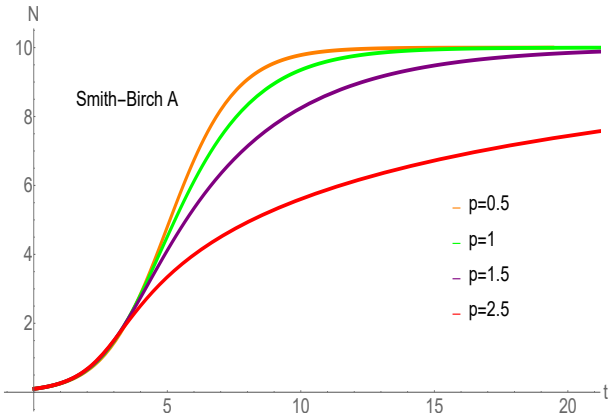

Figure 2. Smith-Birch A model curves with $K = 10$, $N(0.01) = 0.1$, $A = 1$ and $p = 0.5$ (orange), $p = 1$ (green), $p = 1.5$ (purple), $p = 2.5$ (red). Inflection points (numerically calculated) correspond to $N^* = 4.77, 4.14, 3.16, 1.82$, respectively.

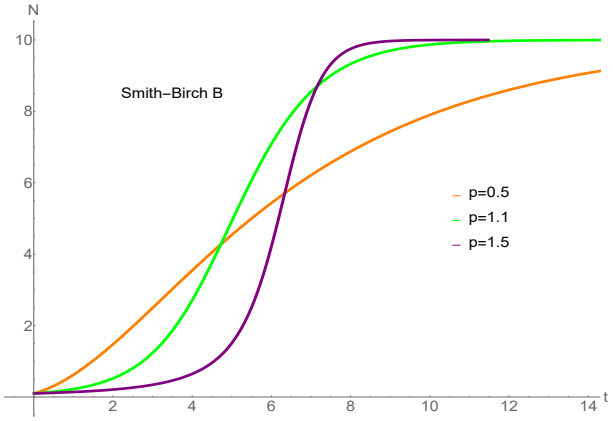

Figure 3. Smith-Birch B model curves with $K = 10$, $N(0.01) = 0.1$, $A = 0.5$ and $p = 0.5$ (orange), $p = 1.1$ (green), $p = 1.5$ (purple). Inflection points (numerically calculated) correspond to $N^* = 3.11, 5.86, 7.11$, respectively.

V. APPLICATIONS

As already mentioned, the traditional SC models listed in the table above do not fit appropriately the time series for the cumulative number of cases during the first 61 days of the COVID 19 pandemic for some countries. In these cases, Birch-Smith, Birch-Smith A or Birch-Smith B are good alternatives to resolve the problem.

The data for the adjusted curves is generated using the function `NonlinearModelFit` from the software Wolfram Mathematica to obtain the optimal values of the parameters. See Appendix II for the detailed methodology and Appendix III for some countries' optimal parameters.

In Figure 4 the results for Kiribati using several sigmoid curves are shown. In this case, the best results correspond to Birch-Smith model.

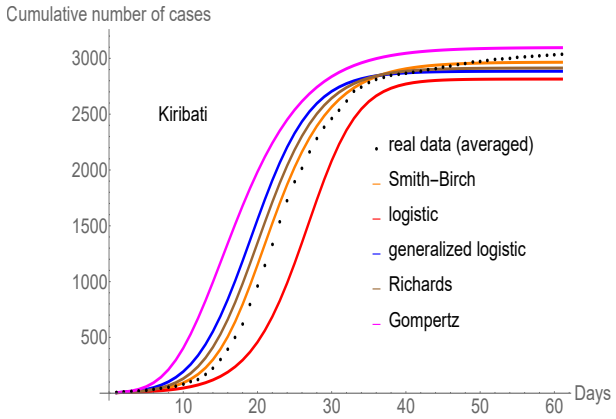

Figure 4. Results for Kiribati using several sigmoid models: Smith-Birch (orange), logistic (red), generalized logistic (blue), Richards (brown) and Gompertz (magenta). The averaged real data is shown in black dots.

In figure 5 the results for Smith-Birch model are shown separately. After the 35-day training period this model produces a good prediction for more than 10 days.

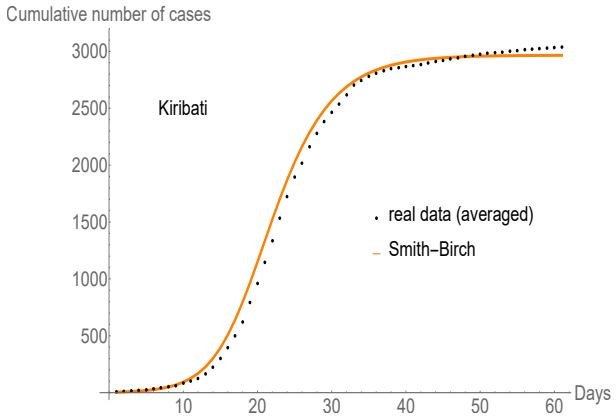

Figure 5. Smith-Birch (orange) results for Kiribati. The averaged real data is shown in black dots.

In figure 6 the results for Palau using several sigmoid models are shown. The best results correspond to Birch-Smith A model. In figure 7 the results for Smith-Birch and Smith-Birch A models are shown separately. Both models fit well during the 35-day training period, but afterwards Smith-Birch A

produces a better prediction for more than 10 days. Similar results are obtained for Somalia (figures 8 and 9).

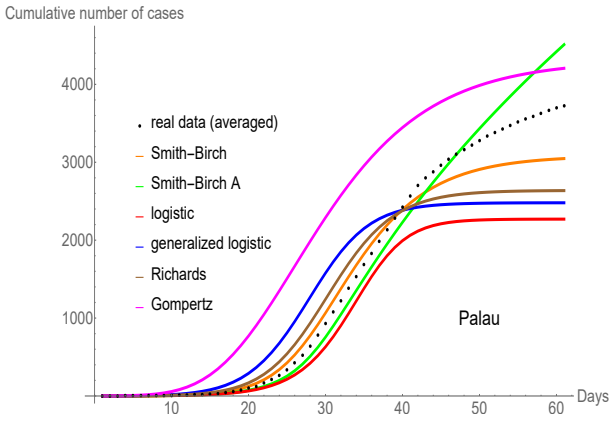

Figure 6. Results for Palau using several sigmoid models: Smith-Birch (orange), Smith-Birch A (green), logistic (red), generalized logistic (blue), Richards (brown) and Gompertz (magenta). The averaged real data is shown in black dots.

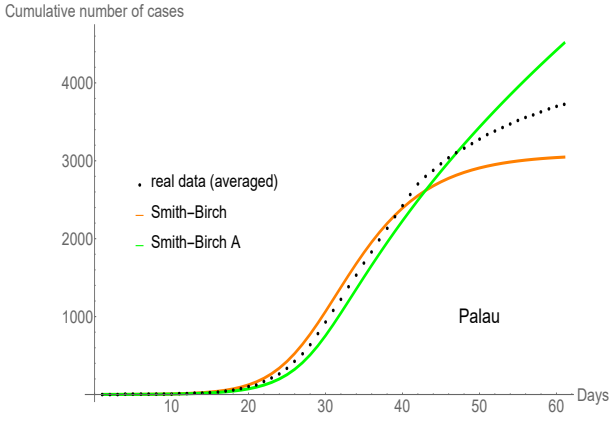

Figure 7. Smith-Birch (orange) and Smith-Birch A (green) results for Palau. The averaged real data is shown in black dots.

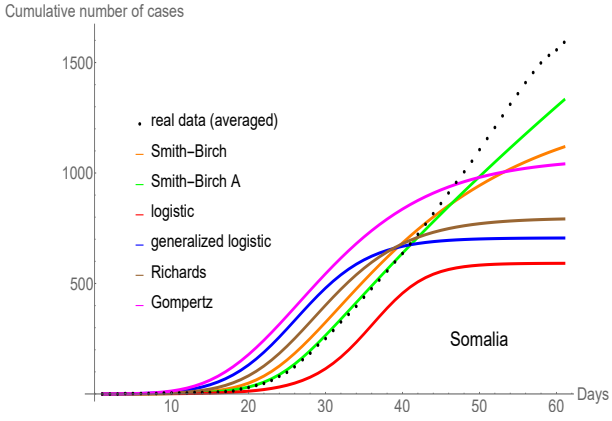

Figure 8. Results for Somalia using several sigmoid models: Smith-Birch (orange), Smith-Birch A (green), logistic (red), generalized logistic (blue), Richards (brown) and Gompertz (magenta). The averaged real data is shown in black dots.

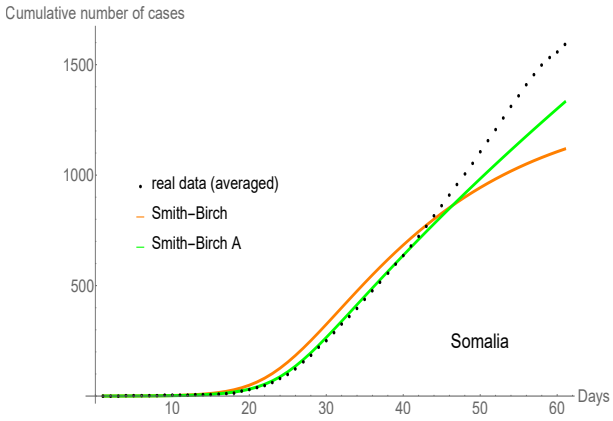

Figure 9. Smith-Birch (orange) and Smith-Birch A (green) results for Somalia. The averaged real data is shown in black dots.

Mauritius is an interesting example. As shown in Figure 10, the carrying capacity was reached in a short time. Smith-Birch A produces good results, although generalized Richards is the best model in this case. Smith-Birch, on the contrary, is a bad choice. In Figure 11 this curves are shown separately.

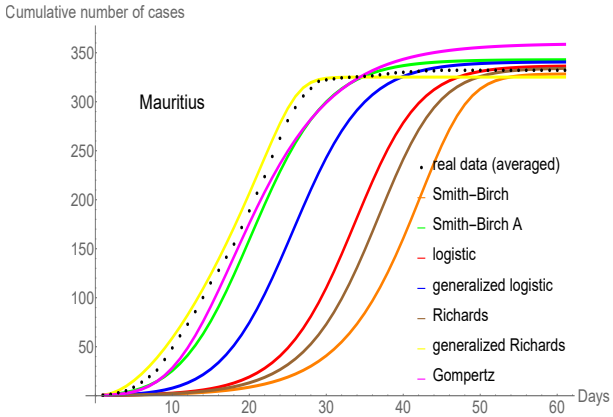

Figure 10. Results for Mauritius using several sigmoid models: Smith-Birch (orange), Smith-Birch A (green), logistic (red), generalized logistic (blue), Richards (brown), generalized Richards (yellow) and Gompertz (magenta). The averaged real data is shown in black dots.

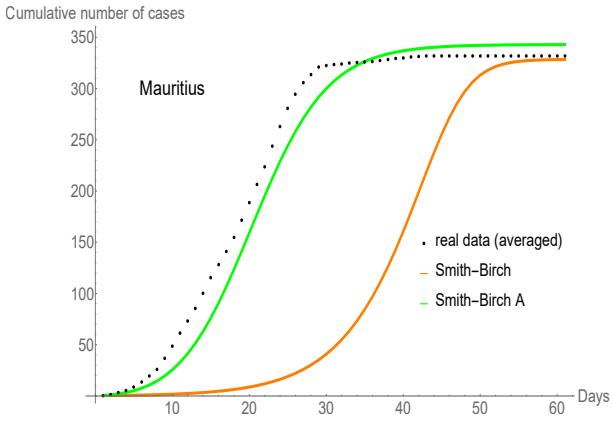

Figure 11. Smith-Birch (orange) and Smith-Birch A (green) results for Mauritius. The averaged real data is shown in black dots.

In [44] it was proven by an statistical analysis that for Cuba data the best model is generalized Gompertz. However, it is interesting to evaluate the performance of Smith-Birch

models in this case. Figures 12 and 13 show good results for Smith-Birch A model, although Smith-Birch and Smith-Birch B results are not satisfactory.

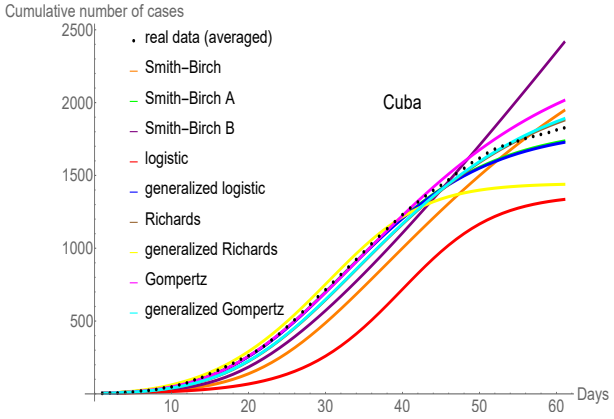

Figure 12. Results for Cuba using several sigmoid models: Smith-Birch (orange), Smith-Birch A (green), Smith-Birch B (purple), logistic (red), generalized logistic (blue), Richards (brown), generalized Richards (yellow), Gompertz (magenta) and generalized Gompertz (cyan). The averaged real data is shown in black dots.

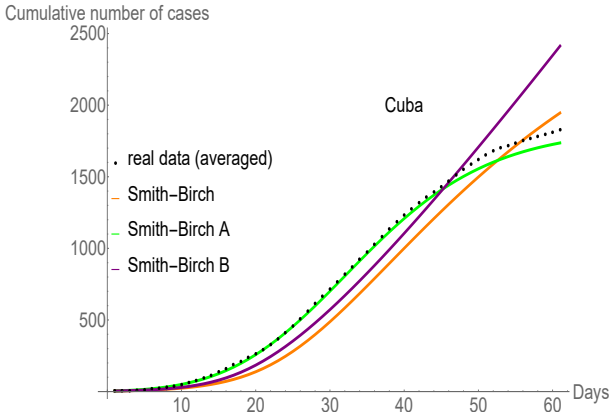

Figure 13. Smith-Birch (orange), Smith-Birch A (green) and Smith-Birch B (purple) results for Cuba. The averaged real data is shown in black dots.

The results for Cambodia using several sigmoid models are shown in Figure 14. In this case, the best model is Smith-Birch B. In Figure 15 it is shown separately, along with Smith-Birch (for comparison).

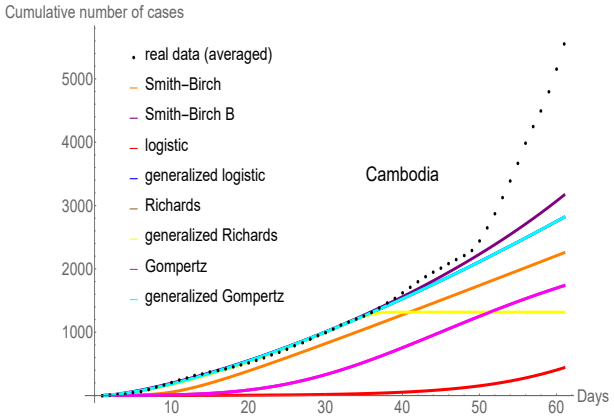

Figure 14. Results for Cambodia using several sigmoid models: Smith-Birch (orange), Smith-Birch B (purple), logistic (red), generalized logistic (blue), Richards (brown), generalized Richards (yellow), Gompertz (magenta) and generalized Gompertz (cyan). The averaged real data is shown in black dots.

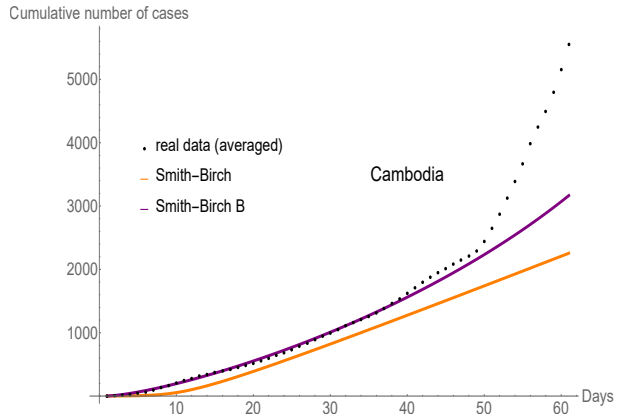

Figure 15. Smith-Birch (orange) and Smith-Birch B (purple) results for Cambodia. The averaged real data is shown in black dots.

VI. CONCLUSIONS

Two new, four-parameter sigmoid curves are introduced, as generalizations of the Smith-Birch model, a member of the logistic family. Analytic and numerical description of these two models are presented. The applicability of the new models for predicting early dynamics of infectious diseases is shown in the case of epidemiologic data from the COVID-19 pandemic in countries where traditional models failed to predict. Due to the wide variety of phenomena which can be described using sigmoid curves, further applications in other areas can be expected, for example, prediction curves of any kind as envelopes of sigmoid curves.

VII. ACKNOWLEDGEMENTS

MTPM acknowledges financial support from COIC/STIA/10104 /2024 and PAPIIT DGAPA UNAM IN101822 projects and hospitality received at Unidad Académica del IIMAS en el Estado de Yucatán, Universidad Nacional Autónoma de México. JBC appreciates the support of the PROEC/UFS/Brazil through the PRAPG Program No. 23038.003836/2023-39 of the Coordination for the Improvement of Higher Level Personnel (CAPES).

VIII. APPENDIX I: ANALYTIC SOLUTIONS FOR THE TSOULARIS GENERALIZED LOGISTIC, SMITH-BIRCH, SMITH-BIRCH A AND SMITH-BIRCH B MODELS

The Tsoularis generalized logistic model (4) with the initial condition $N(t_0) = N_0$ has the solution

$$r(t-t_0) = \begin{cases} \frac{1}{\beta\gamma}\left(\frac{1-\left(\frac{N}{K}\right)^{-\beta}}{1-\left(\frac{N}{K}\right)^{\beta}}\right)^{\gamma} F(\gamma,\gamma,\gamma+1,\left(\frac{N}{K}\right)^{-\beta})\Big|_{N_0}^{N} & \text{if } \alpha = 1 \\ \frac{N^{1-\alpha}}{\alpha-1} F(\frac{1-\alpha}{\beta},\gamma,1+\frac{1-\alpha}{\beta},\left(\frac{N}{K}\right)^{\beta})\Big|_{N_0}^{N} & \text{if } \alpha \neq 1 \end{cases} \tag{8}$$

where

$$F(a,b,c,z) = \frac{\Gamma(c)}{\Gamma(a)\Gamma(b)} \sum_{n=0}^{\infty} \frac{\Gamma(a+n)\Gamma(b+n)}{\Gamma(c+n)} \frac{z^n}{n!} \tag{9}$$

is the hypergeometric function [59].

The Smith-Birch A model (6) with the initial condition $N(t_0) = N_0$ has the solution

$$r(t-t_0) = \left(\frac{A}{Kp} N^p F(1,p,1+p,\frac{N}{K}) + \ln\left(\frac{N}{K-N}\right) \right)\Big|_{N_0}^{N} \tag{10}$$

The Smith-Birch B model (7) with the initial condition $N(t_0) = N_0$ has the solution

$$r(t-t_0) = \begin{cases} \ln\left(\frac{N}{(K-N)^{A+1}}\right)\Big|_{N_0}^{N} & \text{if } p = 1 \\ \left(\frac{A+1}{K}\ln\left(\frac{N}{K-N}\right) - \frac{1}{N}\right)\Big|_{N_0}^{N} & \text{if } p = 2 \\ \left(\frac{A}{K(2-p)} N^{2-p} F(1,2-p,3-p,\frac{N}{K}) + \right. & \\ \left. + \frac{1}{1-p} N^{1-p} F(1,1-p,2-p,\frac{N}{K})\right)\Big|_{N_0}^{N} & \text{if } p \neq 1,2 \end{cases} \tag{11}$$

It should be noted that the solution of the Smith-Birch model (5) is included in (10) and (11) when $p = 1$.

IX. APPENDIX II: METODOLOGY FOR TIME SERIES ANALYSIS

As the number of cases is typically reported at regular time intervals (daily, weekly, etc.), it is reasonable to use mathematical models whose solutions are defined over time discrete domains, so we will use discrete difference equations, instead of first-order differential equations on a continuous time domain, for describing the dynamics of the disease. A classical review on the theoretical and applied scope of first-order difference equations can be found in [60]. A didactic introduction to the study of these equations appears, for instance, in [61].

The standard way of obtaining a difference equation from a continuous one is through the transformation:

$$N(t) \to N_i, \quad \frac{dN}{dt} \to \frac{N_{i+1} - N_i}{h}, \tag{12}$$

where i represents the i-th value of the time series of n_0 length $\{N_i\}_{i=1}^{n_0}$ and h is the time step between recorded values (we are assuming that it is constant). The next steps are

1. The time series $\left\{N_i^0\right\}_{i=1}^{n_0}$ is averaged with a 7 day long moving window, resulting in the time series $\{N_i\}_{i=1}^{n}$, where $n = n_0 - 6$. This smoothing has the effect of eliminating factors like delays in reporting due to the accumulation of unreported cases. This kind of window averaging has been used before in COVID-19 literature [62].

2. From the time series $\{N_i\}_{i=1}^{n}$ the first n_1 elements are used to train each model (calibration period) and form the list of pairs $\{(N_i, N_{i+1})\}_{i=1}^{n_1-1}$.

3. The list of pairs is fitted to the model $Y = X + hg_{\mathbf{\Pi}}(X,i)$, by using the function `NonlinearModelFit` from the software Wolfram Mathematica. From here we obtain the optimal values of the parameters and store them as components of the optimal parameters vector $\mathbf{\Pi}^\star$.

4. The predicted time series $\left\{N_i^\star\right\}_{i=1}^{n}$ is computed through the `RecurrenceTable` function using the optimal values $\mathbf{\Pi}^\star$ and $N_1^\star = N_1$.

X. APPENDIX III: OPTIMAL VALUES FOR THE PARAMETERS FOR SOME COUNTRIES.

Palau:

Model	r	K	A	p
Smith-Birch	0.33	3082.82	1.43	–
Smith-Birch A	0.29	$1.65 \cdot 10^6$	6.07	1.80

Cambodia:

Model	r	K	A	p
Smith-Birch	1.67	13399.3	599.63	–
Smith-Birch B	8.82	$1.37 \cdot 10^{15}$	$1.81 \cdot 10^{11}$	0.23

REFERENCES

[1] V. Vieira, *Comput. ecol. softw.* **10**, 162 (2020).
[2] F. H. Eeckman and W. J. Freeman, *Brain Res.* **557**, 13 (1991).
[3] K. Sandberg, B. M. Bibby, B. Timmermans, A. Cleeremans, and M. Overgaard, *Conscious. Cogn.* **20**, 1659 (2011).
[4] D. R. F. Paul E. Smaldino, Lucy M. Aplin, *Sci. Rep.* **8**, 14015 (2018).
[5] J. M. J. Murre, *Psychon. Bull. Rev.* **21**, 344 (2014).
[6] C. L. T. D. Tab Rasmussen, *J. Hum. Evol.* **23**, 159 (1992).
[7] H. Qiu, K. Durand, H. Rabinovitch-Chable, M. Rigaud, V. Gazaille, P. Clavère, and F. G. Sturtz, *Biotechniques* **42**, 355 (2007).
[8] S. Pixton and R. Howe, *J. Stored. Prod. Res.* **19**, 1 (1983).
[9] A. G. A. Anna M. Michałowska-Kaczmarczyk and Tadeusz Michałowski, *J. Anal. Sci.*, Methods and Instrumentation **4**, 27 (2014).
[10] C. Y. Hsieh, S. L. Fang, Y. F. Wu, Y. C. Chu, and B. J. Kuo, *Hortic.* **7**, 537 (2021).

[11] S. H. Austin, T. R. Robinson, W. D. Robinson, and R. E. Ricklefs, *Methods Ecol. Evol.* **2**, 43 (2011).

[12] M. Michalczu, K. Damaziak, and A. Goryl, *Ann. Anim. Sci.* **16**, 65 (2016).

[13] L. Cao, P.-J. Shi, L. Li, and G. Chen, *Symmetry* **11**, 204 (2019).

[14] T. Onoda, R. Yamamoto, K. Sawamura, Y. Inoue, A. Matsui, T. Miyake, and N. Hirai, *J. Equine Sci.* **22**, 37 (2011).

[15] Y. Zhang, A. Biswas, and V. I. Adamchuk, *Geoderma* **289**, 1 (2017).

[16] K. Hufkens, R. Ceulemans, and P. Scheunders, *Ecol. Inform.* **3**, 97 (2008).

[17] B. G. Akre and D. M. Johnson, *J. Anim. Ecol.* **48**, 703 (1979).

[18] J. I. Lehr Brisbin and M. C. Newman, *Water Air Soil Poll* **57-58**, 691 (1991).

[19] L. A. Kuznar and W. G. Frederick, *Ecol. Econ.* **46**, 296 (2003).

[20] I. McGowan, *The Statistician* **35**, 73 (1985).

[21] K. Kobayashi, W. A. Borders, S. Kanai, K. Hayakawa, H. Ohno, and S. Fukami, *Appl. Phys. Lett.* **119**, 132406 (2021).

[22] D. S. Paolino and M. P. Cavatorta, *Fatigue Fract. Engng. Mater. Struct.* **36**, 316 (2012).

[23] M. El-Khawaga, S. El-Badawy, and A. Gabr, *Arabian J. Sci. Eng.* **45**, 3973 (2020).

[24] S. Mastilović, *Theor. Appl. Mech.* **45**, 95 (2018).

[25] D. Jang, G. Chae, and S. Shin, *Sens.* **15**, 25385 (2015).

[26] B. Lu, H. He, H. Yu, H. Wang, G. Li, M. Shi, and Dongpu, *Sens.* **20**, 7197 (2020).

[27] D. Kucharavy and R. D. Guio, *Procedia Eng.* **9**, 559 (2011).

[28] R. Bürger, G. Chowell, and L. Y. Lara-Díaz, *Math. Biosci.* **334** (2021), ISSN 18793134.

[29] F. Brauer, C. Castillo-Chavez, and Z. Feng, *Mathematical Models in Epidemiology*, Texts in Applied Mathematics (Springer, New York, NY, 2019).

[30] G. Zhou and G. Yan, *Emerg. Infect. Dis.* **9** (2003), ISSN 10806040.

[31] B. Pell, Y. Kuang, C. Viboud, and G. Chowell, *Epidemics* **22** (2018), ISSN 18780067.

[32] D. W. Shanafelt, G. Jones, M. Lima, C. Perrings, and G. Chowell, EcoHealth **15** (2018), ISSN 16129210.

[33] L. Dinh, G. Chowell, K. Mizumoto, and H. Nishiura, *Theor. Biology Med. Model.***13** (2016), ISSN 17424682.

[34] S. Zhao, S. S. Musa, H. Fu, D. He, and J. Qin, *Parasit. Vectors.* **12** (2019), ISSN 17563305.

[35] B. Malavika, S. Marimuthu, M. Joy, A. Nadaraj, E. S. Asirvatham, and L. Jeyaseelan, *Clin. Epidemiol. Glob. Health.* **9** (2021), ISSN 22133984.

[36] C. Y. Shen, IJID **96** (2020), ISSN 18783511.

[37] K. Wu, D. Darcet, Q. Wang, and D. Sornette, *medRxiv* (2020).

[38] G. L. Vasconcelos, A. M. Macêdo, R. Ospina, F. A. Almeida, G. C. Duarte-Filho, A. A. Brum, and I. C. Souza, *PeerJ* **2020** (2020), ISSN 21678359.

[39] K. Roosa, Y. Lee, R. Luo, A. Kirpich, R. Rothenberg, J. M. Hyman, P. Yan, and G. Chowell, *J. Clin. Med.* **9** (2020), ISSN 20770383.

[40] K. Roosa, Y. Lee, R. Luo, A. Kirpich, R. Rothenberg, J. M. Hyman, P. Yan, and G. Chowell, *Infect. Dis. Model.* **5** (2020), ISSN 24680427.

[41] Y. Wu, L. Zhang, W. Cao, X. Liu, and X. Feng, *Front. Phys.* **8**, 566 (2021), ISSN 2296-424X.

[42] M. López, A. Peinado, and A. Ortiz, *PLoS ONE* **16** (2021), ISSN 19326203.

[43] P. Pincheira-Brown and A. Bentancor, *Epidemics* **37** (2021), ISSN 18780067.

[44] M. T. Pérez-Maldonado, J. Bravo-Castillero, R. Mansilla, R. O. Caballero-Pérez, *Nova scientia* **14**, 18 (2022).

[45] G. Jarne, J. Sanchez-Choliz, F. Fatas-Villafranca, *Evol. Inst. Econ. Rev.* **3**, 239 (2007).

[46] L. S. Pontriaguin, *Ecuaciones Diferenciales Ordinarias* (Editorial Pueblo y Educación, La Habana, 1981).

[47] M. Carrillo, J. M. González, *Technol. Forecasting Social Change* **69**, 233 (2002).

[48] W. G. Bardsley, R. E. Childs, *Biochem. J.* **149**, 313 (1975).

[49] Z. Li, B. S. Yang Zhang, Z. Xing, Q. Wang, *Electronics* **11**, 1365 (2022).

[50] R. Gomeni, C. Gomeni, *Comput. Biomed. Res.* **13**, 489 (1980).

[51] H. Li, X. Jiang, G. Huo, C. Su, B. Wang, Y. Hu, Z. Zheng, nt. *J. Adv. Manuf. Technol.* **119**, 1531 (2022).

[52] P. Verhulst, *Corr. Math. Physics* **10**, 113 (1838).

[53] A. Tsoularis, J. Wallace, *Math. Biosci.* **179** (2002), ISSN 00255564.

[54] M. H. Zwietering, I. Jongenburger, F. M. Rombouts, K. van't Riet, *Appl. Environ. Microbiol.* **56**, 1875 (1990).

[55] J. Schnute, *Can. J. Fish. Aquat. Sci.* **38**, 1128 (1981).

[56] K. M. C. T. Erve , E. T. Erve, *Ecol. Modell.* **359**, 117 (2017).

[57] F. E. Smith, *Ecol.* **44**, 651 (1963).

[58] C. P. D. Birch, *Ann. Bot.* **83**, 713 (1999).

[59] M. Abramowitz, I. A. Stegun, *Handbook of Mathematical Functions with Formulas, Graphs, and Mathematical Tables* (Dover, New York, 1964), ninth dover printing, tenth gpo printing edition.

[60] R. M. May, *Nature* **261**, 459 (1976), ISSN 20522541.

[61] W. E. Boyce, R. C. DiPrima, *Elementary Differential Equations* (John Wiley & Sons, Inc., Hoboken, NJ, 2012).

[62] A. L. M. J. A. Mesejo-Chiong, Ciencias Matemáticas **34**, 19 (2020).